Crystal stability limits at positive and negative pressures, and crystal-to-glass transitions

Francesco Sciortino,[1,2] Ulrich Essmann,[1,3] H. Eugene Stanley,[1] Mahin Hemmati,[4]
Jun Shao,[4] George H. Wolf[4] and C. Austen Angell[4]

[1] *Center for Polymer Studies and Department of Physics, Boston University, Boston, Massachusetts 02215*
[2] *Dipartimento di Fisica, Università "La Sapienza," Piazzale Aldo Moro 7, 00185 Roma, Italy*
[3] *Department of Chemistry, University of North Carolina, Chapel Hill, North Carolina 27599*
[4] *Department of Chemistry, Arizona State University, Box 871604, Tempe, Arizona 85287-1604*

The direct crystal-to-glass transformation, i.e., spontaneous amorphization, which was first observed by thermal annealing of stishovite SiO_2 at ambient pressure, has now been observed as an isothermal phenomenon during both compression and decompression of initially stable crystals. While counterintuitive, and dependent on kinetically controlled metastable events, the phenomenon is of broad interest and potential importance in materials science and geophysics. In this paper we use a combination of molecular dynamics simulations and analyses of laboratory data to explore the metastable crystal ranges, including the negative pressure range, for key compounds such as the ices, silicas, and alkaline earth perovskites. Our focus is on the establishment of phenomenological patterns rather than on specific metastability-terminating mechanisms. We find that a simple quadratic law, $P - P_s \sim (V - V_s)^2$ (where P_s and V_s are the values of the pressure P and volume V on the spinodal), well approximates the equations of state over much of the metastable and even the stable range—and implies the existence of an isochoric boundary line for stability to isotropic density fluctuations. We delineate the conditions under which amorphization occurs, usually substantially before the stability limit is reached.

PACS number(s): 05.70.Fh

I. INTRODUCTION

There is now a resurgence of interest in phase transitions in out-of-equilibrium materials, dispersed among subjects such as one-phase melting [1,2] tensile strength [2,3] binary alloys and superconductivity [4] and most recently, pressure-induced amorphization [5–17]. Part of the interest derives from the recognition that materials with interesting properties, including high-T_c superconductors, are often materials that exist close to their mechanical stability limits, and are often metastable with respect to other phases. It is becoming clear that, while the majority of individual phases have metastable ranges beyond their thermodynamic stability boundaries, the metastable ranges are not unlimited but rather have absolute boundaries imposed by the arrival at an intrinsic instability (the vanishing of restoring forces) with respect to one or the other type of lattice fluctuation.

Except near absolute zero, the metastability will be relieved by some nucleation and growth process. However, the fluctuations that assist the relevant nucleation barrier crossing process will be those with respect to which the crystal is becoming absolutely unstable since these will be the modes with the greatest anharmonicity. To date the focus of the many studies of this phenomenon has been on identification of the failure mode. For instance, many studies [1,3,4,9,10,16] have suggested that the first mode to go unstable is a shear mode, and this will no doubt often be the case. Given the complexities

of lattice dynamics, however, it seems likely that failure will often be more subtle and may involve, for instance, softening of and/or avoided crossing of optical modes, as demonstrated recently [18] for some silicate perovskites treated in this work, and even coupling of optical modes to acoustic modes.

Recognizing the difficulty of establishing any general mechanisms for failure, we focus our attention here on another important issue. This issue concerns the location of the absolute stability limits in (P, T) space relative to the equilibrium thermodynamic stability boundaries for different polymorphs of the same material. Also of concern is the dependence of such limits on the direction of departure from the thermodynamically stable domain. It is curious that, while enormous interest [6–17] was generated by the observation by Mishima, Calvert, and Whalley [5] of the ice I_h-to-glass transformation under compression, only a few workers [16–20] took account of the earlier, but equally significant, observation of isothermal crystal-to-glass transformation by Liu and Ringwood during decompression of calcium silicate perovskite [21] or of the even earlier observation of amorphization of stishovite SiO_2 on decompression and annealing [22]. With this in mind we present results obtained from a selection of molecular dynamics simulations in which the improbability of nucleation events maximizes the metastable range that can be explored. As a result we observe certain common (but not invariable) phenomena near the limits of metastability. These can be usefully related to phenomena observed in metastable liquids and interpreted

to first order by mean-field theories of condensed matter. These interpretations in turn suggest experiments not yet performed. We report results for both molecular (ices) and ionic (silica and perovskite) materials.

II. ICE I

In the first case studied, that of ice I_h under tension as well as compression, we have used the TIP4P potential and a large primary box, 864 molecules, in order to avoid the danger of suppressing destabilizing modes [23,24]. We have used both constant-volume and constant-pressure (i.e., the variable box shape algorithm) simulations [25]. Details of the simulation are given in Ref. [26]. In the second case, that of ice VIII under de-

compression, a box of 432 molecules has been used and the variable box shape algorithm was employed [25,26].

In our work, we calculate density-pressure relations at a series of temperatures during both increase and decrease of density from zero-pressure values [26]. In ice I, the approach to the metastability limit on compression, for all temperatures below 100 K, and on tension for temperatures below 250 K, is manifested by the onset of rapid but reversible changes in density with increasing pressure in the constant volume simulation, accompanied by small distortions in box shape in flexible box simulations [see Fig. 1(a)]. In the case of increasing tension (negative pressure), approach to the metastability limit is indicated by a similarly increasing compressibility. The failure in this case is manifested by a sharp
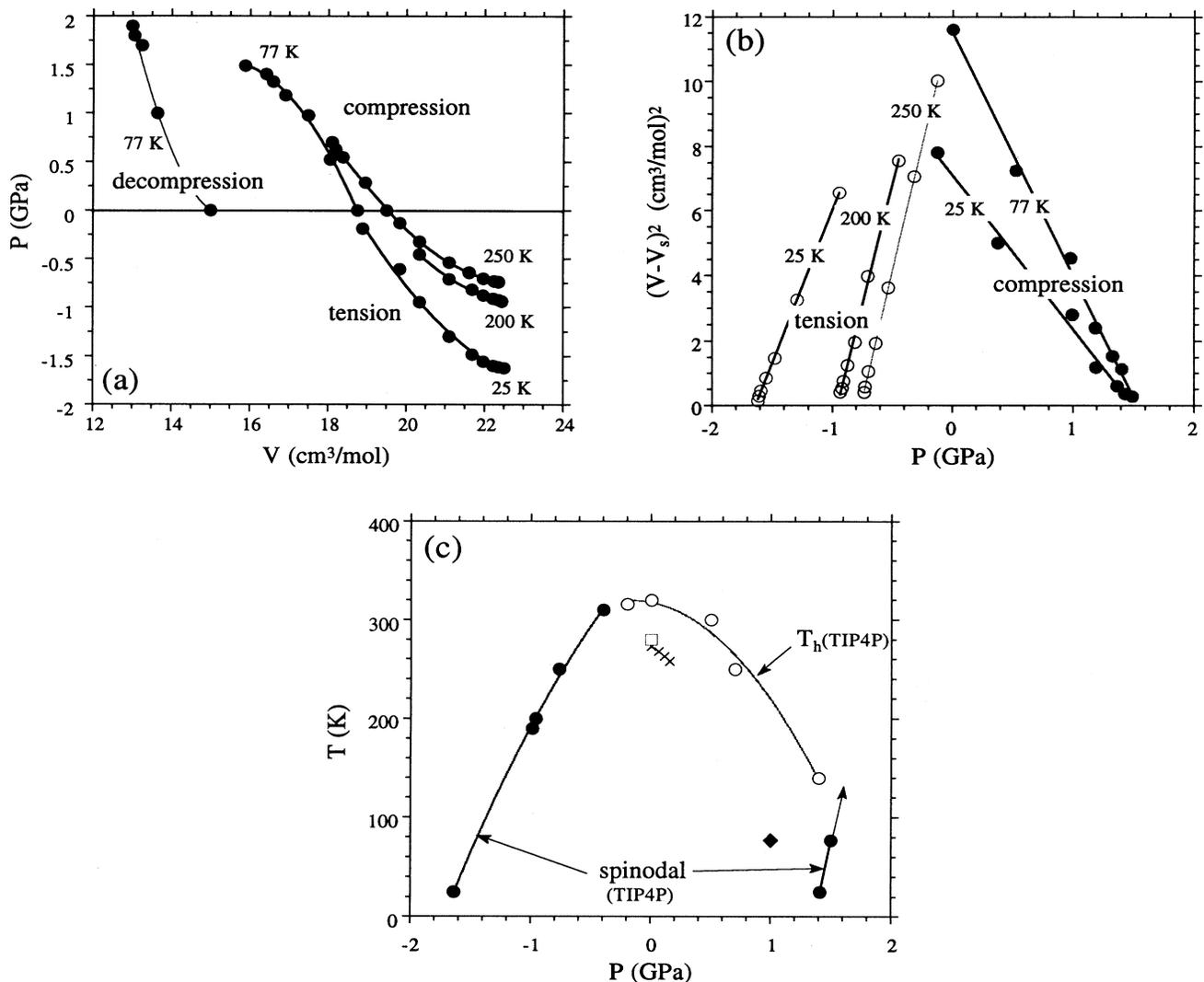

FIG. 1. Ice I_h under compression and tension. (a) P–V relations at several temperatures. Solid lines give the reversible behavior. (b) Tests of mean-field behavior of volume near compression and tension stability limits (P_s, T_s). (c) Values of P_s that linearize the plots in part (b) and define the stability limits under compression (filled circles). Open circles denote the nucleated fusion points (non-spinodal). The open square is the equilibrium melting point at atmospheric pressure, and crosses show the melting line. The diamond shows the laboratory amorphization pressure at 80 K [4].

break in the plot, since P tends rapidly back to zero on rupture. We will see comparable behavior with ice VIII and perovskites under decompression.

The large and growing density fluctuations near the limits of stability in Fig. 1(a) are reminiscent of the behavior observed near the limit of stability in metastable water (both supercooled and superheated). In each of the latter cases increasing compressibilities are observed [27,28], and can be explained by the approach to a spinodal line [29], the position of which is established (in mean field) by equations of state. Since kinetic phenomena, viz., nucleation of new phases, prevent close approach to a spinodal, its absence as a singularity in higher order treatments of phase transitions is not germane to our discussion.

Figure 1(b) demonstrates that the exponents describing this singularity are consistent with those of the classical (mean field) spinodal [29],

$$P - P_s \sim (V - V_s)^2, \qquad (1)$$

where P_s and V_s are the values of the pressure P and volume V on the spinodal. This does not mean that the system ultimately fails by nucleation initiated by isotropic density fluctuations. Studies of SiO_2 quartz [17] and perovskite $CaSiO_3$ [18] show otherwise. Rather, the spinodal sets an upper limit on the pressure (or tension) to which the phase could conceivably exist, hence providing a readily accessible indicator of the stability field for a compound. Use of the variable box shape algorithm can provide some guidance as to the nature of preemptive instabilities since the fluctuations in the entire strain tensor can be evaluated. However, pinning down the precise failure modes and failure pressure will require for each case detailed lattice dynamics analysis of the sort provided in Refs. [16] and [18]. We note, in the present case of ice I, that the box shape at 77 K, like the pressure, was reversible up to the failure pressure of 14 kbar, quite close to the spinodal limit of 16 kbar.

We found the constant-volume results and the flexible box results to be similar. The difference, a slightly earlier collapse in the flexible box case, is in the direction expected though it is barely outside calculation errors, in view of the different method of accounting for the long-range Coulomb forces and the different ensembles used in the simulation.

We show below that, in the decompression of ice VIII, the same simple mean-field quadratic law may be applied, both to the simulation results and to the experimental observations of Hemley *et al.* [30].

The overall behavior for ice I_h can be summarized in the metastable phase diagram, Fig. 1(c). Figure 1(c) shows the complete mechanical stability region in the (T, P) plane [16]. The picture is similar to that conceptualized by Ponyatovsky and Barkalov [31] for different polymorphs of a substance, although it will be seen that it is not general. Note that at high temperature under tension, metastable melting of ice preempts cavitation. Indeed, on increasing the temperature at $P = -0.2$ GPa, the crystal first transforms to the liquid phase at 311 K. Then the metastable liquid cavitates near 340 K.

III. ICE VIII

Ice VIII is the stable structure of ice formed at pressures above 1.5 GPa. Oxygen atoms in ice VIII are positioned in two interpenetrating ice I_c sublattices. Even
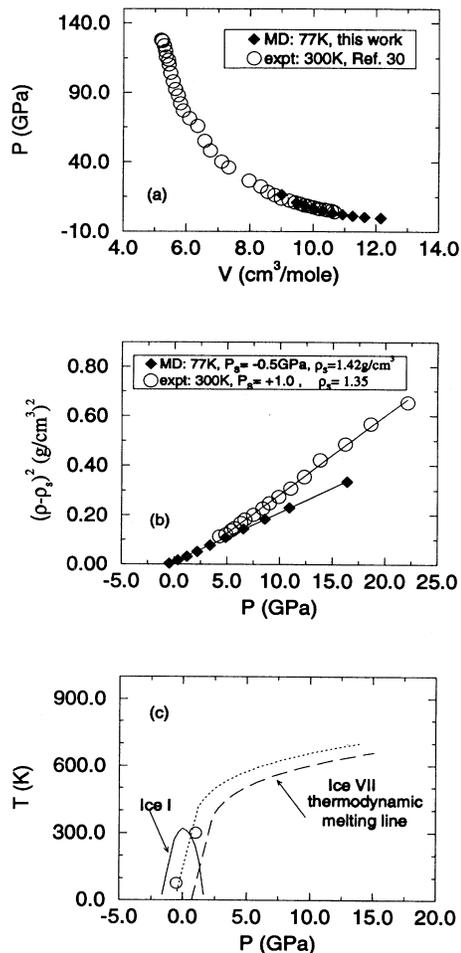

FIG. 2. Ices VII and VIII under decompression. (a) P-V relations for ice VII from experiments at ambient temperature [30], and simulations of TIP4P ice VIII at 77 K (this work). (b) Tests of the quadratic law for ices VII and VIII. Best fit parameters for the data ranges shown are given in the legend. A negative pressure stability limit at 77 K is in accord with decompression of ice VIII to ambient pressure reported by Klug, Honda, and Tse [20]. Note that we fit the data both in the variables $(V - V_s)^2$ and $(\rho - \rho_s)^2$. The quality of the fit is better in the second variable than the first. For this reason the figure shows the variable $(\rho - \rho_s)^2$, both for experimental data and for simulations. Moreover, the fit using $V - V_s$ gives a positive intercept P_s, which is inconsistent with the experimental observation of Klug, Honda, and Tse [20]. (c) Loci of stability limits for ice polymorphs to isotropic fluctuations according to quadratic law for ice I from Fig. 1(c) combined with those of ice VIII from Fig. 2(b) (open circles) and a conjecture (dotted line) based on the high-pressure melting line, from Ref. [46], shown as a dashed line.

though each molecule has eight nearest neighbors it forms hydrogen bonds only to the four neighbors on its own sublattice.

In Fig. 2(a) we show the (P, V) relations obtained from constant pressure flexible box simulations for the decompression of ice VIII. In this case the equation of state has been experimentally measured between 128 and 4.3 GPa at 300 K [30] and the data are included in Fig. 2(a). Since the expansivity is very small the temperature difference affects the volume minimally, hence the agreement is seen to be good, particularly at lower pressures. The experimental data between 60 GPa and ambient pressure conform, within experimental error, to a quadratic law [see Fig. 2(b)]: $P - P_s \sim (\rho - \rho_s)^2$. The limiting pressure obtained from this fitting is +1.0 GPa at a density of 1.35 g/cm^3. Klug, Handa, and Tse [20] confirm that ice VIII under decompression at 77 K does not amorphize but their further experiments with annealing schedules imply that amorphization under isothermal decompression would occur at 125 K.

Our simulation data also conform to a quadratic law in the variable $\rho - \rho_s$ with $P_s = -0.5$ GPa and $\rho_s = 1.42$ g/cm^3, as shown in Fig. 2(b).

It is interesting that ice VIII, which requires such high pressures to become thermodynamically stable, should have a metastable domain extending at low temperatures into the negative pressure. Our study of this phase is in its initial stages but we combine knowledge of the melting lines with some speculation to propose in Fig. 2(c) the larger picture in which the metastable domains for different polymorphs of the same substance are jointly displayed in what we might call a Ponyatovsky-Barkalov diagram [31]. The stability field of ice VIII is very large and will evidently only be terminated at ultrahigh pressure by collapse to a metallic state. Of obvious interest are the intermediate cases of ice II and ice VI, which should have similar high-pressure, as well as low-pressure, limits.

IV. SIO$_2$ CRISTOBALITE

Findings from a less extensive molecular dynamics (MD) study of a cristobalitelike SiO$_2$ are summarized in Fig. 3. In this case the diverging compressibility is only obvious under tension [Fig. 3(a)] where the log-log plots familiar to critical point phenomenology are seen [Fig. 3(b)] to be linear over three orders of magnitude with exponent 0.5. The behavior under compression is ambiguous even at low temperatures perhaps because the failure mechanism is a shear instability as in quartz [17] and the coupling of shear fluctuations to volume fluctuations is weak. The break points on compression, however, are well defined up to high temperatures.

Results are summarized in Fig. 3(c), which differs from Fig. 1(c) by using a volume coordinate for reasons we now discuss.

V. PHENOMENOLOGICAL TRENDS, STRUCTURAL OBSERVATIONS, AND RELATION TO LABORATORY STUDIES

Some phenomenological trends for these two very different substances can be noted. So long as no liquid

phase can form, we find that the failure occurs or tends to occur at a critical volume V_s, which is independent of temperature, in contrast to spinodals associated with critical points [32]. The calculated V_s values for ice I_h
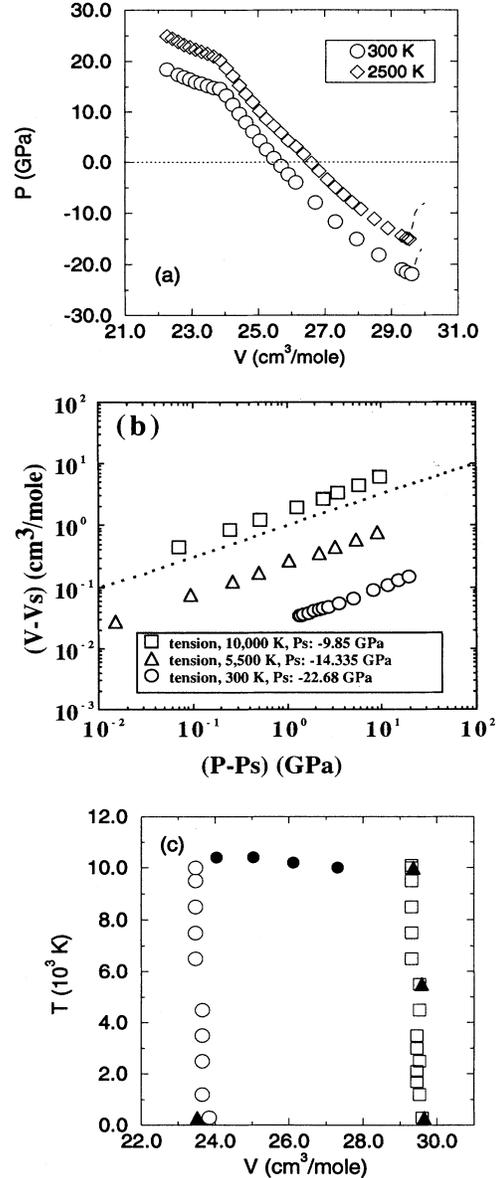

FIG. 3. SiO$_2$ cristobalite under compression and tension (a) P–V relations; the 2500 K curve has been displaced upward 5 GPa for clarity. (b) Log-log plots of $V - V_s$ against $P - P_s$ showing linearization with mean-field exponent 0.5 (dotted line). (c) Limiting volumes under compression and tension plotted against volume [note distinction from Fig. 1(c) to emphasize isochoric limits to metastability under compression (open squares), and tension (open circles). Filled circles denote nucleated melting points, and filled triangles denote V_s obtained from power-law fits of part (b). In the case of the simulated "cristobalite," the collapse at 300 K occurs 25% below the pressure of the laboratory phenomenon (22 GPa [8]): our potential function is too approximate for accurate predictions on SiO$_2$.

are always 22.7 cm^3/mol under stretch and 15.8 cm^3/mol (below 100 K [14]) under compression. Cristobalite always collapses if extended to 29.7 cm^3/mol or compressed to 23.4 cm^3/mol [see Fig. 3(c)] [33]. Such an "isochoric metastability boundary" has been noted [2] (by Born instability) for the simple embedded atom potential and for Lennard-Jones systems under tension.

A comment on the structural character of TIP4P ice I_h at the 77 K stability limit is needed. The radial distribution function (RDF) shows the growth during compression of intensity at about 0.35 nm, the position of the "fifth neighbor" in the liquid phase [34]. At the highest density from which the compression is reversible (and the original crystal is recovered on decompression), this shoulder is on the verge of becoming a maximum. Near this condition, the RDF peaks are very broad, more similar to those of the glass than of the crystal, although no irreversible changes have occurred. The crystal is presumably in a state in which a large, but subcritical, number of molecules occupy defect sites. At this point, a fluctuation such as that occurring at about time step 20 000 in Fig. 2 of Ref. [9(b)] can nucleate an irreversible collapse to the glass. However, until such a fluctuation occurs, the system is metastable and can be recovered in its original state on slow decompression [35]. The latter behavior can be contrasted with that under tension, where no defect buildup is seen and where quadratic laws apply to much higher temperatures. The distinction must lie in the differences in energy barriers to critical nucleus formation under compression and tension. Indeed, the energy lost in deforming the linear hydrogen bonds on compression is compensated by the energy gain due to the increased number of neighbors. Such compensation is not possible on stretching, where direct rupture of linear hydrogen bonds is a prerequisite for failure.

In laboratory studies, ice I_h transforms to a pressure-vitrified phase near 1.0 GPa at 77 K [5] [marked by a square in Fig. 1(c)]. This pressure is significantly lower than the spinodal pressure observed in this MD study, but this is not surprising since the time scale for laboratory observation is some 10 orders of magnitude longer than that of the simulation. On laboratory time scales the transition at 77 K will occur by homogeneous nucleation and growth of amorphous domains via optical mode softening, as is observed in electron microscopic studies of the pressure-induced amorphization of quartz-structured GeO$_2$ [8].

Laboratory detection of prespinodal increases in response functions in ice would probably also be precluded at 77 K by the nucleation event, in the same way that divergent behavior is not observed in our simulations of ice at higher temperatures [Fig. 1(a)] due to the fact that, even on the computer time scale, the probability of crossing the nucleation barrier becomes very high during the simulation. This observation is important in connection with the search for signs of spinodal failure in laboratory pressurized crystals. It suggests that experiments should be conducted at the lowest possible temperature in order to avoid masking of divergences by preemptive homogeneous nucleation.

So far, we have shown that crystalline structures

described by four different potentials (this work and Ref. [2]) all exhibit an "isochoric metastability boundary" under both tension and compression, a remarkable and provocative observation.

VI. METASILICATE PEROVSKITES

We now look at additional cases of how crystalline phases created at very high pressures relieve their metastability on isothermal decompression. We follow up on the Liu and Ringwood [21] observation that perovskite CaSiO$_3$, created in a diamond anvil cell experiment, collapses to a glassy state on decompression (which was of great frustration to them but great interest to us).

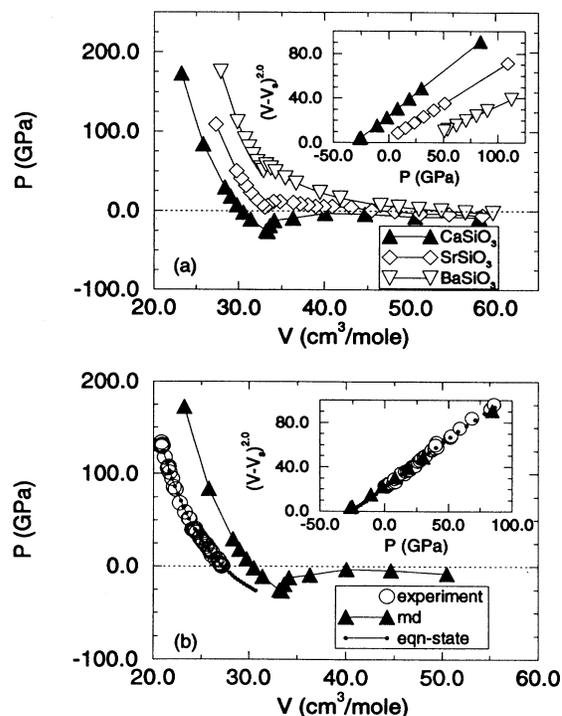In Fig. 4 we examine this case to test the expectation

FIG. 4. (a) Variation of pressure with volume during decompression of simulated alkaline earth metasilicate perovskites M[II]SiO$_3$. Note how a change of cation size parameter shifts the spinodal limit on perovskite stability from positive to negative pressures without changing the limiting volume. The inset shows how data over a wide volume range are consistent with the existence of a spinodal limit slightly beyond the observed rupture point (for CaSiO$_3$, $P_s = -30.8$ GPa, $V_s = 35.3$ cm^3; SrSiO$_3$, $P_s = -6.1$ GPa, $V_s = 35.7$ cm^3; BaSiO$_3$, $P_s = 48.6$ GPa, $V_s = 36.1$ cm^3). (b) Variation of pressure with volume for laboratory and simulated CaSiO$_3$. The limitation of the rigid ion potential as parametrized by us is manifested by a discrepancy in the pressure. However, the curvatures are comparable since the quadratic plots testing the mean field stability limit [inset of (b)] superimpose. Quantitative agreement is obtainable with modified potentials based on those of Matsui for MgSiO$_3$ (see [18]).

that the failure will again be preceded by diverging density fluctuations (preempted, in the case of laboratory experiments, by homogeneous nucleation). The data plotted in Fig. 4 were obtained, using MD simulations with the transferable rigid ion model (TRIM) potentials from earlier studies [36], on crystals of group IIA metal silicate perovskites [M(II)SiO$_3$] on which many experimental and theoretical studies have been made [11,37–39]. A more detailed study, using refined potentials that better reproduce the experimental data, has been reported elsewhere [18] but the simple TRIM potential simulations produce the same phenomenological trends and are more than adequate for our present purposes.

The equations of state obtained for these crystalline phases [see Fig. 3(a)] are qualitatively similar to those for ice VIII and for SiO$_2$ cristobalite under tension, Figs. 2 and 3, although in the cases of SrSiO$_3$ and BaSiO$_3$ the pressure never reaches negative values before the failure occurs. In the three cases in which the stable crystal has our cubic box symmetry, Fig. 3 shows that the quadratic law $P - P_s \sim (V - V_s)^2$ is well obeyed. The value of V_s proves to be almost the same, 35–36 cm^3/mol, for all cases, notwithstanding the different cation radii. The latter strongly affect the rupture pressure. Further expansion of CaSiO$_3$ beyond the V_s to the ambient pressure glass volume, 40 cm^3/mol [40], results in a disordered product [41]. However, in short time simulations, unlike experiment, this product has not lost its memory of the crystal from which it was derived. Recompression to crystal volume results in the reformation of the perovskite crystal. To obtain irreversible transformation to the glassy state found by Liu and Ringwood [21], an additional extension of volume to 50 cm^3/mol, followed by recompression, or annealing at $T > 600$ K, is needed.

It is now known that it is possible with care to recover the cubic perovskite phase at ambient temperature, though it vitrifies within a few hours at ambient temperature [37]. MgSiO$_3$, as is well known, can always be recovered at ambient temperature, and then persists indefinitely. The calculations suggest therefore that the SrSiO$_3$ and BaSiO$_3$ perovskites will only be observable under static high pressure conditions.

In Fig. 4(b) and its inset, we show that the curvature in the experimental equation of state for CaSiO$_3$ obtained by Mao et al. [38] is comparable with our findings although our equation of state is displaced to higher pressures (reflecting the same deficiency in the TRIM potential parameters discussed in Ref. [41]. For the Fig. 4 inset presentation of experimental data, we use a V_s value of 32.0 cm^3/mol obtained from the extremum in the Birch-Murnagahn equation of state used by Mao et al. [38] to fit their data. A quadratic plot of the experimental data points then gives a behavior almost indistinguishable from our MD findings. Finally, we emphasize that with reparametrization of CaSiO$_3$ pair potentials, based on those of Matsui for MgSiO$_3$ perovskite [42], we can obtain quantitative agreement with the experimental data. These calculations, combined with detailed lattice dynamics calculations to identify the complex cascade of

instabilities responsible for the final collapse of the crystal to the glassy state, are described elsewhere [18]. Reference [18] also shows that, as in the case of ice I_h and SiO$_2$ cristobalite, the low-pressure boundary is isochoric.

VII. CONDITIONS FOR AMORPHIZATION

From the foregoing we can define certain conditions that need to be fulfilled before isothermal crystal-to-amorphous transformations can be expected. First and most obvious, the crystal needs to reach its stability boundary while the pressure is positive or only weakly negative, so that the alternative failure to a cracked or cavitated state does not preempt the more isotropic amorphization process. Second, it must occur at a temperature below the glass transition temperature of the amorphous phase so that nucleation of a thermodynamically stable crystal phase does not permit a bypassing of the amorphous domain of configuration space. Finally, initial crystal structure must not be such that there is a continuous nondiffusive (displacive) path to a stable crystalline state of lower free energy than that of the glass.

The actual path to amorphization may well be via intermediate crystalline states which themselves have no mechanical stability at the temperature and volume of the primary crystal failure as found for CaSiO$_3$ perovskite [18]. As emphasized earlier, the crystal will almost invariably find some path to failure before the density fluctuation divergence limit, indicated by the equation of state, can be reached. It is only a surprise that in the case of ice I_h the latter can be so closely approached.

VIII. CONCLUDING REMARKS

The study of metastable domains in crystalline materials and the vitrification process that is frequently encountered on passing the stability limit, appears to be a rich field for future work. The field includes metal-to-amorphous semiconductor transitions [31] and molecular insulator-to-amorphous semiconductor (or to amorphous metal) transitions [11]. As a subclass the recently recognized amorphous-amorphous [8,43-45] transitions could be included. Near the metastable limits, particularly at low temperatures (ambient for strongly bound systems), many interesting phenomena may be anticipated.

ACKNOWLEDGMENTS

[1] Reviewed by L. L. Boyer, Phase Transitions **5**, 1 (1985).

[2] J. Wang, S. Yip, S. R. Phillipott, and D. Wolf, J. Alloys Compounds **194**, 407 (1993); Phys. Rev. Lett. **71**, 4182 (1993).

[3] R. L. B. Selinger, Z.-G. Wang, A. Ben-Shaul, and W. M. Gelbart, J. Chem. Phys. **95**, 9128 (1991).

[4] H. J. Fecht, G. Han, Z. Fu, and W. L. Johnson, J. Appl. Phys. **67**, 1744 (1990); J.-B. Suck (private communication).

[5] D. Mishima, L. D. Calvert, and E. Whalley, Nature **310**, 393 (1984).

[6] R. J. Hemley, A. P. Jephcoat, H. K. Mao, L. C. Ming, and M. H. Manghnani, Nature **334**, 52 (1988); R. J. Hemley, L. C. Chen, and H. K. Mao, *ibid.* **338**, 638 (1989).

[7] Q. Williams, R. Knittle, R. Reichlin, S. Martin, and R. Jeanloz, Science **249**, 647 (1990).

[8] G. H. Wolf *et al.*, in *High Pressure Research: Applications to Earth and Planetary Sciences*, edited by Y. Syono and M. H. Manghani (Terra Scientific, Tokyo, 1992).

[9] (a) J. S. Tse and M. Klein, J. Chem. Phys. **92**, 3992 (1990); (b) J. S. Tse and D. D. Klug, Phys. Rev. Lett. **67**, 3559 (1991); (c) J. S. Tse, J. Chem. Phys. **96**, 5482 (1992).

[10] D. D. Klug, Y. P. Handa, J. S. Tse, and E. Whalley, J. Chem. Phys. **90**, 2390, (1989).

[11] S. Sugai, J. Phys. C **18**, 799 (1985).

[12] Y. Fujii, M. Kowaka, and A. Onadera, J. Phys. C **18**, 789 (1985).

[13] A. Jayaraman, D. L. Wood, and R. G. Maines, Phys. Rev. B **35**, 8316 (1987).

[14] J. H. Nguyen, M. B. Kruger, and R. Jeanloz, Phys. Rev. B **49**, 3734 (1994).

[15] G. C. Serghiou, R. R. Winters, and W. S. Hammack, Phys. Rev. Lett. **68**, 3311 (1992).

[16] N. Binggeli and J. R. Chelikowsky, Phys. Rev. Lett. **69**, 2220 (1992); N. Binggeli, N. R. Keskar, and J. R. Chelikowsky, Phys. Rev. B **49**, 3075 (1994).

[17] V. F. Degtyareva, I. T. Belash, E. G. Ponyatovsky, and V. I. Rashupkin, Fiz. Tverd. Tela (Leningrad) **32**, 1429 (1990) [Sov. Phys. Solid State **32**, 834 (1990)].

[18] M. Hemmati, A. Chizmeshya, G. H. Wolf, P. H. Poole, J. Shao, and C. A. Angell, Phys. Rev. B **51**, 14841 (1995).

[19] P. Richet, Nature **331**, 56 (1988).

[20] D. D. Klug, Y. P. Handa, and J. S. Tse, J. Chem. Phys. **90**, 2390 (1989).

[21] L.-G. Liu and A. E. Ringwood, Earth Planet. Sci. Lett. **28**, 209 (1975).

[22] B. J. Skinner and J. J. Fahy, J. Geophys. Res. **68**, 5595 (1963).

[23] We have maintained internal consistency in our rigid box calculations. All allowed strain fluctuations involve maximum wavelengths of about the same value. Although in the constant volume simulations we do not allow infinite wavelength fluctuations, as in constant pressure simulations [9], the large size of the simulation box does not suppress strain fluctuations with wavelengths shorter than about 9 molecules. Comparison with our constant pressure variable box shape results described herein prove this is adequate. In laboratory ice, one expects that the longest wavelength fluctuations drive the instability; however, the loss of stability at shorter wavelengths (those sampled in our simulation) will produce generically identical failures at slightly higher pressures.

[24] Small scale simulations produce restrictions on the range and type of general strain fluctuations that such simulations allow. For example, with a small cell of only 128 molecules, box constraints allow infinite wavelength fluctuations in the strain tensor elements s_{11}, $s_{22} + s_{33}$, and $s_{12} + s_{13}$. However, the maximum wavelength fluctuations allowed for s_{44}, s_{14} and for s_{12}, s_{13}, s_{22}, and s_{33} separately is a dimension of only about 5 molecules. The validity of calculations with such samples needs to be independently verified. A true mechanical instability has not yet been properly documented in ice I_h; certain moduli have only been observed to vanish during the transition, hence as a result of, rather than being involved in its initiation. Since no lattice dynamics calculations have yet been performed for ice I_h, the exact origin of the instability is as yet unresolved. It remains an intriguing question because such data as exist on the elastic constants of ice I_h do not suggest an early vanishing of the shear modulus.

[25] W. Smith, modified version of computer program MD-SPC4 of the CCP5 Program Library.

[26] For ice I_h, the protons of the 864 water molecules are positioned so as to produce a disordered structure with zero dipole moment. Simulations are performed for periods of time ranging from 30 ps far from the transition point to 100 ps close to the transition point. The last 20 ps were used for analysis in all cases. In our initial constant volume studies of ice I_h compression under constant volume, the reaction field method is used to handle the long-range interactions. Checks at $T = 77$ K show no significant differences in (P, V) relations between Ewald summation and reaction field. The constant pressure simulations have been performed with the Parinello-Rahman technique and with the Ewald summation, but for 432 molecules. In response to the external pressure the box cannot only change its volume isotropically, but any deformation of the simulation box (including changes of the angles between the box edges) is allowed. This technique has, in particular, been employed in studies of crystal transformations. The details of the method are described in S. Nose and M. L. Klein, Mol. Phys. **50**, 1055 (1983). Run lengths were between 50 and 300 ps. Points on the phase diagram in Fig. 1 for T other than 250, 200, 77, and 25 K (for which the long NVT runs are performed) are obtained by monitoring the density pressure relationship in simulation at constant volume and/or pressure during very slow temperature scans (0.2 K/ps). In a less exhaustive study of cristobalitelike SiO_2, we use 192 ions in a cubic box in the NVT ensemble simulated with a two-term rigid ion potential suggested by J. Kieffer (private communication) to stabilize the crystal. Each plotted point derives from a 10-ps run, and points are spaced more closely as the spinodal is approached.

[27] C. A. Angell, Annu. Rev. Phys. Chem. **34**, 593 (1983).

[28] It should be noted that ice in compression does not show divergent behavior above about 100 K because of prior homogeneous nucleation of the liquid phase.

[29] R. J. Speedy, J. Phys. Chem. **86**, 3002 (1982).

[30] R. J. Hemley, A. P. Jephcoat, H. K. Mao, C. S. Zha, L. W. Finger, and D. E. Cox, Nature **330**, 737 (1987).

[31] E. G. Ponyatovsky and O. I. Barkalov, Materials Sci. Rep. **8**, 147 (1992).

[32] Q. Zheng, D. J. Durben, G. H. Wolf, and C. A. Angell,

Science **254**, 829 (1991).

[33] While the product of the compression collapse of the simulated cristobalite phase is disordered, it is not clear if "amorphization" is the most appropriate description since a defective chromium vanadate structure is also a possible product [S. Tsuneyuke, Y. Matsui, H. Aoki, and M. Tsukada, Nature **339**, 209 (1989)].

[34] F. Sciortino, A. Geiger and H. E. Stanley, Phys. Rev. Lett. **65**, 3452 (1990).

[35] Our proposal of diverging compressibility associated with runaway defect populations is close in concept to the explanation of boundaries on crystal stability domains by J. W. Cahn [Trans. Metal. Soc. AIME **242**, 166 (1967)]. We emphasize the analogy to the spinodal limit for stretched liquids: all that is needed for a spinodal instability is an inflection in the free energy versus pressure. In neither the liquid nor the crystal case can the equation of state spinodal be reached—even in principle—because the lengthening time scale for internal equilibration (critical slowing down) must eventually cross the critical nucleation time scale, with the inevitable consequence. Our work shows, however, that the spinodal can be closely approached in a variety of cases.

[36] C. A. Angell, P. A. Cheeseman, and S. Tamaddon, Science **218**, 885 (1982); C. A. Angell, P. A. Cheeseman, and R. R. Kadiyala, Chem. Geol. **62**, 85 (1987); C. A. Angell, C. Scamehorn, C. C. Phifer, R. R. Kadiyala, and P. A. Cheeseman, Phys. Chem. Minerals **15**, 221 (1988).

[37] R. J. Hemley, M. D. Jackson, and R. G. Gordon, Phys. Chem. Miner. **14**, 2 (1987); R. J. Hemley and R. E. Cohen, Ann. Rev. Earth Planet. Sci. **20**, 553 (1992).

[38] H. K. Mao, L. C. Chen, R. J. Hemley, A. P. Jephcoat, Y.

Wu, and W. A. Bassett, J. Geophys. Res. **94**, 889 (1989).

[39] M. Kanzaki, J. F. Stebbins, and X. Xue, Geophys. Rev. Lett. **18**, 463 (1992).

[40] O. V. Mazurin, M. V. Streltsina, and T. P. Shvaikovskaya, in *Handbook of Glass Data, Part A: Silica Glass and Binary Silicate Glasses* (Elsevier, Amsterdam, 1983), p. 466.

[41] The calculations with TRIP potentials yield an Si—O coordination number (CN) of 4.6 for this glass, which is actually smaller than the value, 4.8, obtained by melting the same ensemble at 6000 K and 40 cm^3/mol and isochorically quenching to 300 K. However, both CN's are higher than the value 4.0 characterizing the laboratory glass and the pressures are also much higher than ambient. This discrepancy is consistent with the overestimate of the equation of state for $CaSiO_3$ shown in Fig. 4(b), and demonstrates that these potentials need to be modified. Refinements based on the Matsui pair potentials for $MgSiO_3$ perovskite (see Ref. [42]) lead to excellent agreement with the equation of state for the $CaSiO_3$ perovskite, and to glasses which have Si—O coordination numbers of 4.05, consistent with the experiments.

[42] M. Matsui, Phys. Chem. Minerals **169**, 234 (1988).

[43] O. Mishima, J. Chem. Phys. **100**, 5910 (1994).

[44] P. H. Poole, F. Sciortino, U. Essmann, H. E. Stanley, Nature **360**, 324 (1992); P. H. Poole, U. Essmann, F. Sciortino, and H. E. Stanley, Phys. Rev. E **48**, 4605 (1993).

[45] C. A. Angell, Science **267**, 1924 (1995).

[46] O. Mishima and S. Endo, J. Chem. Phys. **68**, 4417 (1978).